

## **General Disclaimer**

### **One or more of the Following Statements may affect this Document**

- This document has been reproduced from the best copy furnished by the organizational source. It is being released in the interest of making available as much information as possible.
- This document may contain data, which exceeds the sheet parameters. It was furnished in this condition by the organizational source and is the best copy available.
- This document may contain tone-on-tone or color graphs, charts and/or pictures, which have been reproduced in black and white.
- This document is paginated as submitted by the original source.
- Portions of this document are not fully legible due to the historical nature of some of the material. However, it is the best reproduction available from the original submission.

RIGIDITY OF LATTICE DOMES

V. A. Savelyev

(NASA-TM-75387) RIGIDITY OF LATTICE DOMES  
(National Aeronautics and Space  
Administration) 29 p HC A03/MF A01 CSCL 20K

N79-20393

Unclas

G3/39 17103

Translation of "Ustoychivost' setchatykh kupolov",  
Metallicheskiye Konstruktsii, Moscow, Stroyizdat, 1966,  
pp. 325 - 339



NATIONAL AERONAUTICS AND SPACE ADMINISTRATION  
WASHINGTON, D.C. 20546

MARCH 1979

## RIGIDITY OF LATTICE DOMES

V. A. Savelyev

/325\*

We will examine a lattice dome with a triangular lattice (fig. 1). The dome has a spherical shape, in the sense that it is a polyhedron inscribed in a sphere of radius  $R$ .

We will assume that all of the rods are rectilinear and hinged in multiple joints. A load  $P$  is applied to each of the multiple joints.

With a ratio  $\frac{H}{d} > \frac{1}{5}$ , the dome belongs to the category of gently sloping domes; therefore, the change in the lengths of the rods and the angles between the rods can be disregarded.

We will examine the simplest and most likely form of the loss of rigidity, which consists of the simultaneous staving in towards the center of curvature of certain multiple joints of the domed lattice surface. These multiple joints are designated with the letter  $A$  in figure 2.

We will assume that the dome has initial irregularities of shape, which consist of a radial deviation  $f_0$  of the multiple joints  $A$  from the spherical surface.

We will compose the equations of equilibrium of multiple joints  $A$  and  $C$  (fig. 3), and determine  $N_1$  and  $N_2$ :

---

\*Numbers in the margin indicate pagination in the foreign text.

$$N_1 = \frac{P}{6\beta} \cdot \frac{1}{1 - \zeta_0 - \zeta} \quad (1)$$

$$N_2 = \frac{P}{6\beta} \cdot \frac{1 - 3\zeta_0 - 3\zeta}{1 - \zeta_0 - \zeta} \quad (2)$$

Here,  $\zeta_0 = \frac{\varphi_0}{\beta}$  and  $\zeta = \frac{\varphi}{\beta}$  are dimensionless parameters of the initial and supplementary sags.

The length of rod 1 prior to loading is equal to

$$l_0 = \sqrt{c^2 + (h - F_0)^2} = c \sqrt{1 + \left(\frac{h - F_0}{c}\right)^2} = c \sqrt{1 + (g^2(\beta - \varphi_0))}, \quad (3)$$

and under a load

$$l = \sqrt{(c - u)^2 + (h - F_0 - F)^2} = c \sqrt{1 - \frac{2u}{c} + \frac{(h - F_0 - F)^2}{c^2}} = c \sqrt{1 - \frac{2u}{c} + (g^2(\beta - \varphi_0 - \varphi))}. \quad (4)$$

As a result of the smallness of the angle  $\beta$ , one can approximately assume that

$$l_0 \approx c \left[ 1 + \frac{1}{2} (\beta - \varphi_0)^2 \right] = c \left[ 1 + \frac{\beta^2}{2} (1 - \zeta_0)^2 \right]; \quad (5)$$

$$l \approx c \left[ 1 + \frac{1}{2} (\beta - \varphi_0 - \varphi)^2 \right] - u \approx c \left[ 1 + \frac{\beta^2}{2} (1 - \zeta_0 - \zeta)^2 \right] - u. \quad (6)$$

The displacement of multiple joint C, evoked by deformation of rod 2, is designated by u:

$$u \approx N_2 \frac{c}{EF}. \quad (7)$$

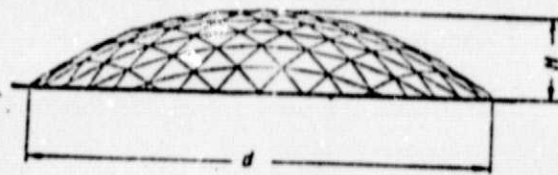


Fig. 1. Diagram of gently-sloping lattice dome

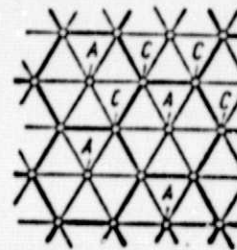
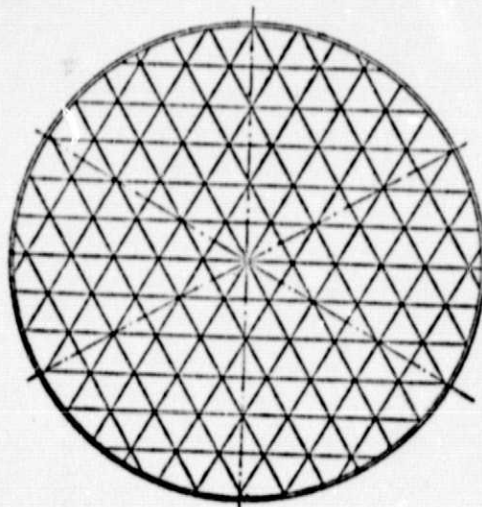


Fig. 2. Simplest form of loss of rigidity of lattice surface

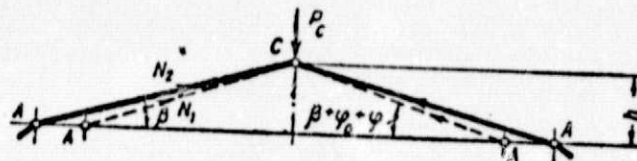
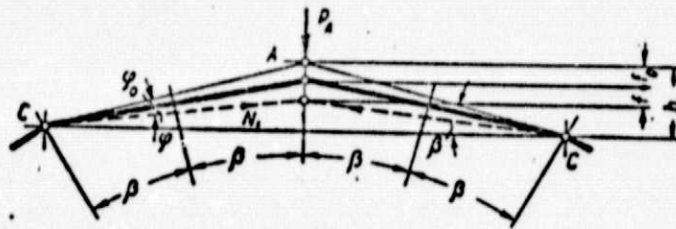


Fig. 3. Deformation of multiple joints A and C of a lattice dome

The relative shortening of rod 1 is

$$\epsilon_1 = \frac{l_0 - l}{l_0} = \frac{\beta^2}{2} (2\zeta - 2\zeta_0\zeta - \zeta^2) + \frac{u}{c}. \quad (8)$$

This shortening corresponds to the load  $P$ , which is equal to

$$P = 2\beta(1 - \zeta_0 - \zeta)EF\epsilon_1; \\ P = 2EF\beta^2 \frac{\zeta(1 - \zeta_0 - \zeta)(2 - 2\zeta_0 - \zeta)}{2(\zeta_0 + \zeta)}. \quad (9)$$

Expression (9) determines the total nonlinear dependence of the magnitude of the force, applied to multiple joint A, on the parameter of sag of this multiple joint  $\zeta$ , with regard for the initial deviation  $\zeta_0$ .

We will examine first the ideal system ( $\zeta_0 = 0$ ):

$$P = 2EF\beta^2 \frac{1}{2} (2 - 3\zeta + \zeta^2). \quad (10)$$

Assuming that the sags are small, as compared with  $h$ , i.e.,  $\zeta \ll 1$ , we obtain the critical surface load

$$P_n = 2EF\beta^2. \quad (11)$$

We will introduce the designation  $P = \frac{P}{P_n}$ . From expression (10)

$$\bar{P} = \frac{1}{2} (2 - 3\zeta + \zeta^2). \quad (12)$$

The diagram of the equilibrium states of an ideal system

is shown in figure 4 by the bold-face line. With an increase in the sags, the load falls to the lower critical point, and then begins to increase again.

We will investigate the effect of the initial deviations on the magnitude of the critical load. Shown in figure 4 are the curves which correspond to different values of  $\zeta_0$ . From the very beginning of loading, the system behaves as a nonlinear system. If the initial sag is directed toward the center of curvature, then, with an increase in the initial deviations, the parameter of the upper critical load decrease quickly. With  $\zeta_0 = 1$ , the lower point disappears, i.e., the danger of sudden cracking through drops; however, the deformability of such a system is extraordinarily great. In multiple joints which are structurally impossible to implement in the form of ideal joints, considerable overstresses may occur. With  $\zeta_0 = 2$ , the initial situation corresponds to a supposed cracked-through state of the ideal dome. The diagram of equilibrium corresponds precisely to the branch of rigid supercritical equilibrium shapes of an ideal dome ( $\zeta_0 = 0$ ).

The geometric parameter

$$\beta = \frac{l_0}{2R}. \quad (13)$$

is contained in the formula of the upper critical load (11).

In domes with a small radius of curvature, the angle  $\beta$  has large values, and the critical loads are sufficiently great. Therefore, for small domes, the greatest danger is not the total loss, but the local loss of rigidity—the bulging of individual rods. With an increase in the span of the dome, the angle  $\beta$  decreases, and the magnitude of the

critical load drops sharply. A total loss of rigidity becomes more likely.

We will pose the problem of determining at what values of  $\beta$  and, roughly, at which dimensions of the dome the total loss of rigidity becomes decisive.

We will first assume that the dome has an ideal spherical shape. Then, the force in rod 1, with a load  $P_k$ , will be equal to

$$N_k = \frac{P_k}{6\beta} = \frac{EF}{3} \beta^3. \quad (14)$$

By setting expression (14) equal to the Eulerian critical force, we obtain /329

$$\beta_1 = \pi \sqrt{\frac{3}{\lambda}}, \quad (15)$$

and for a maximal  $\lambda=150$

$$\beta_1 = 0,0363. \quad (16)$$

If  $\beta < \beta_1$ , then the total loss of rigidity occurs; if  $\beta > \beta_1$ , then an individual rod loses its rigidity first.

The actual structures always have initial imperfect shapes. The radial deviation of multiple joint A from the designed position can occur as a result of the inaccuracy of manufacture of the rods 1. The normal accuracy of manufacture of the metallic structures for the rods from 2 to 6 m in length is

$$\delta = \left( \frac{1}{2000} + \frac{1}{3000} \right) l_0.$$



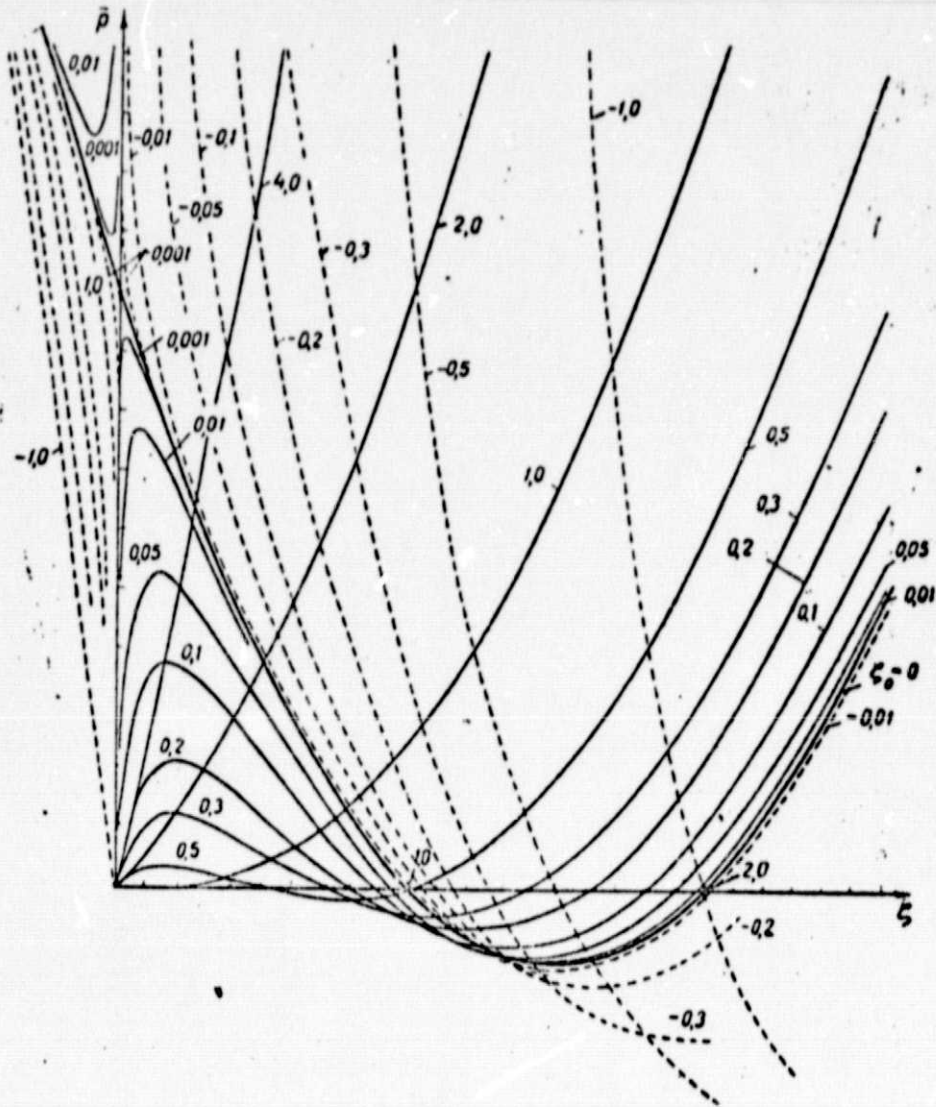


Fig. 4. Diagrams of equilibrium states of a spherical dome with different initial spans

By utilizing expressions (5) and (6), it is not difficult to obtain the dependence which associates the parameters  $\beta$  and  $\xi_0$  with  $\delta/\lambda_0$ :

$$\beta = \sqrt{\frac{\delta}{l_0} \cdot \frac{2}{2\epsilon_{\text{пр}}^2 - \epsilon_0^2}}. \quad (17)$$

ORIGINAL PAGE IS  
OF POOR QUALITY

By equating the critical forces in rod 1, with a local and total loss of rigidity, we will obtain the following, similar to expression (15):

$$\beta = \frac{\pi\sqrt{3}}{\lambda} \sqrt{\frac{1 - \zeta_0 - \zeta_k}{P_k}}. \quad (18)$$

Here,  $\zeta_k$  is the resilient sag, which corresponds to  $\bar{P}_k$ .

By solving equations (17) and (18) together, utilizing the graphs in figure 4, we obtain, for  $\lambda=150$ ,

$$\beta_1 \approx 0.05 \text{ or } R \leq 10\%. \quad (19)$$

For example, with a rod length  $l_0=3$  m, the radius of curvature of a single-layer lattice spherical dome should not exceed  $R_1=30$  m, in order to avoid a total loss of rigidity.

How can one increase the rigidity of large-span domes?

An increase in the rod length  $l_0$  in order to ensure condition (19) is economically unsuitable, since it leads to an increase in the flexibility of individual rods, and weighting of the structure of the roofing.

Apparently, a more successful structural approach, which increases the total rigidity, is the creation of large initial deviations of individual multiple joints of the dome in the direction opposite to the expected bulging, which makes it possible to utilize the branches of rigid equilibrium conditions with negative values of  $\zeta_0$  (dotted lines in the graphs in figure 4).

One can also give the dome a sort of cracked-through shape in advance. In this case, the load—sag dependences also have the form of rigid ascending curves ( $\zeta_0=2$ ;  $\zeta_0=4$ ).

The steel dome in Baton Rouge (USA), designed by R. B. Fuller, which is 118 m in diameter, can serve as an example of the practical utilization of such methods. It is made up of hexagonal sheet panels, each of which is specially given a convex shape.

330

Of course, these methods can not serve as a total solution of the problem of rigidity of domes with such satisfactorily large spans. With an increase in  $\beta$ , the danger of cracking through increases according to more complex (than those examined) forms of bulging, which encompass a considerably greater section of the lattice surface. In addition, it is necessary to note that an artificial break in the outline of the

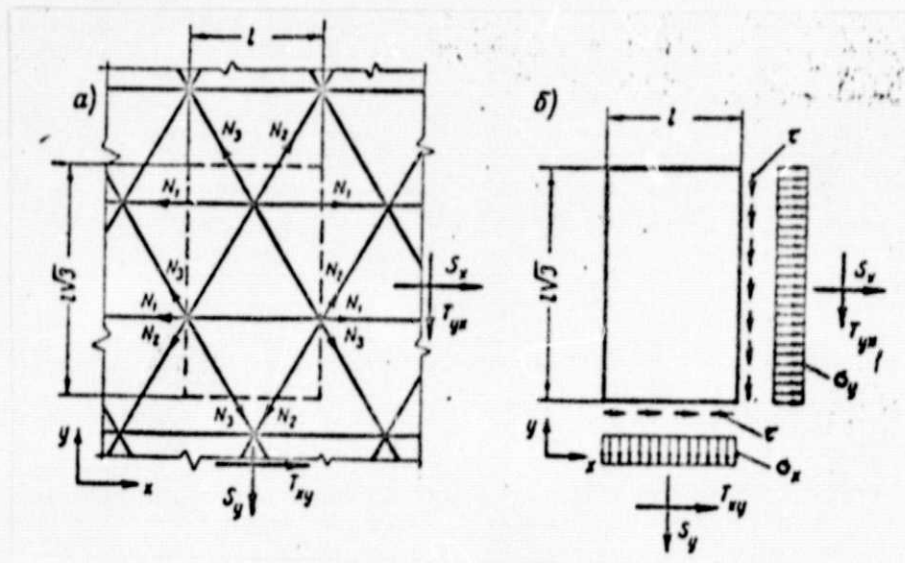


Fig. 5. Comparison of stressed state of a section of a:  
a—lattice surface; b—solid casing

bearing surface of the dome structure introduces an irregularity into the distribution of forces among the rods, which considerably reduces its economical effectiveness.

A more all-purpose method for increasing the rigidity of large-span domes is the creation of three-layer lattice structures, which consist of two lattice surfaces, interconnected by a lattice. With radii of curvature which considerably exceed the lengths of the rods, it is advisable to view such structures as solid shells, rather than rod systems.

A three-layer lattice dome, according to the nature of its operation, is equivalent to some three-layer shell with a light filler. The role of the external bearing layers is played by the lattice surfaces, while the role of the filler is fulfilled by the connective lattice, which operates only under shear stress.

In order to bring a uniform triangular lattice to a solid shell, we shall examine the stressed state of a section of the lattice surface, which has the shape of a rectangle with sides  $l$  and  $\sqrt{3}l$  (fig. 5,a). This section is the minimum section which reflects the discrete nature of the lattice structure. We will assume that, within the limits of this section, the forces in the rods in one direction are equal. By comparing the resultants of the normal and tangential components of the forces applied to this section with the corresponding resultants for a solid rectangle of the very same dimensions, with a thickness  $t$  (fig. 5,b), we obtain

$$\left. \begin{aligned} \sigma_x &= \frac{2}{\sqrt{3}l} \left[ N_1 + \frac{1}{4} (N_2 + N_3) \right]; \\ \sigma_y &= \frac{\sqrt{3}}{2l} (N_2 + N_3); \\ \tau &= \frac{1}{2l} (N_3 - N_2). \end{aligned} \right\} \quad (20)$$

In that particular case where  $\sigma_x = \sigma_y = \sigma$ ;  $\tau = 0$

ORIGINAL PAGE IS  
OF POOR QUALITY

$$N_1 = N_2 = N_3 = \frac{1}{\sqrt{3}} l \sigma.$$

We will investigate the deformation of an elementary rod triangle.

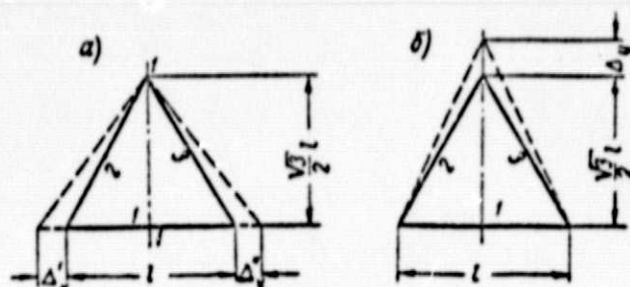


Fig. 6. Diagram of deformation of an elementary rod triangle  
a—in the direction of the x axis; b—in the direction of the y axis

We will first assume that the deformation occurs only in the direction of the x axis, while in the direction of the y axis, the rods do not change their length, i.e.,  $\epsilon_x = \Delta_x / l$ , and  $\epsilon_y = 0$ , with  $\Delta_x = \Delta_x' + \Delta_x''$ . The axis 1—1 will be considered fixed (fig. 6,a).

The length of rod 2, prior to deformation, is equal to  $l$ , and after deformation

$$l_2 = \sqrt{\left(\frac{l}{2} + \Delta_x'\right)^2 + \frac{3l^2}{4}} = \sqrt{l^2 + l\Delta_x' + \Delta_x'^2}$$

or, with accuracy up to terms on the order of  $\Delta_x'^2$ ,

$$l_1 = l \left( 1 + \frac{\Delta'_x}{2l} \right);$$

similarly

$$l_2 = l \left( 1 + \frac{\Delta''_x}{2l} \right).$$

We will determine the relative lengthenings of the rods:

$$\epsilon_1 = \frac{\Delta'_x + \Delta''_x}{l} = \epsilon_x; \quad (21)$$

$$\epsilon_1 = \frac{\Delta'_x}{2l}; \quad \epsilon_2 = \frac{\Delta''_x}{2l} \quad \text{or} \quad \epsilon_1 + \epsilon_2 = \frac{\epsilon_x}{2}. \quad (22)$$

In the general case

/332

$$\Delta'_x \neq \Delta''_x; \quad \epsilon_1 - \epsilon_2 \neq 0,$$

i.e., shift of the lattice takes place towards

$$\delta = \frac{\Delta'_x - \Delta''_x}{2}.$$

We will designate the shift angle through  $\gamma$ ; then

$$\gamma = \frac{2\delta}{\sqrt{3}l} = \frac{\Delta'_x - \Delta''_x}{\sqrt{3}l},$$

hence

$$\epsilon_1 - \epsilon_2 = \frac{\sqrt{3}}{2} \gamma. \quad (23)$$

We will now examine the deformation of a rod triangle in the direction of the y axis (fig. 6,b).

The lengths and relative lengthenings of the rods after deformation are respectively equal to

$$l_1 = l; \quad l_2 = l_3 = \sqrt{\frac{l^2}{4} + \left(\frac{\sqrt{3}}{2}l + \Delta^2\right)} \approx l \left(1 + \frac{\sqrt{3}}{2} \cdot \frac{\Delta y}{l}\right);$$

$$e_1 = 0; \quad e_2 = e_3 = \frac{\frac{\sqrt{3}}{2} \Delta y}{2l} = \frac{3}{4} e_y. \quad (24)$$

Thus, for two specific cases of deformation of a lattice system

$$e_x \neq 0; \quad e_y = 0;$$

$$e_x = 0; \quad e_y \neq 0$$

the dependences of the magnitudes of  $\epsilon_1$ ,  $\epsilon_2$ , and  $\epsilon_3$  on  $\epsilon_x$ ,  $\epsilon_y$ , and  $\gamma$  are determined.

We will obtain the expressions for the general case of  $\epsilon_x \neq 0$  and  $\epsilon_y \neq 0$ , utilizing the principle of superposition:  $\epsilon_i = \epsilon_{xi}$

$$\left. \begin{aligned} e_2 + e_3 &= \frac{1}{2} (e_x + 3e_y); \\ e_2 - e_3 &= \frac{\sqrt{3}}{2} \gamma. \end{aligned} \right\} \quad (25)$$

Generally speaking, rods 1, 2, and 3 can be made from different materials and have different cross-sectional areas. In this case, the equivalent solid shell will be anisotropic. We will limit our investigation to the simplest case:

$$E_1 = E_2 = E_3 = E; \quad F_1 = F_2 = F_3 = F$$

In this case, one can write

$$N_1 = e_1 EF; \quad N_2 = e_2 EF; \quad N_3 = e_3 EF.$$

We will substitute these values into formula (20):

$$\left. \begin{aligned} \sigma_x &= \frac{2}{\sqrt{3} h} EF \left[ e_1 + \frac{1}{4} (e_2 + e_3) \right]; \\ \sigma_y &= \frac{\sqrt{3}}{2h} EF (e_2 + e_3); \\ \tau &= \frac{1}{2h} EF (e_2 - e_3). \end{aligned} \right\} \quad (26)$$

Utilizing formula (25), we will write the relations (26) in the form

$$\left. \begin{aligned} \sigma_x &= \frac{3}{4h} \sqrt{3} EF \left( e_x + \frac{1}{3} e_y \right); \\ \sigma_y &= \frac{3}{4h} \sqrt{3} EF \left( \frac{1}{3} e_x + e_y \right); \\ \tau &= \frac{\sqrt{3}}{4h} EF \gamma. \end{aligned} \right\} \quad (27)$$

The corresponding expressions for the stresses with a planar stressed state of an isotropic shell have the form

$$\left. \begin{aligned} \sigma'_x &= \frac{E'}{1-\mu^2} (e_x + \mu e_y); \\ \sigma'_y &= \frac{E'}{1-\mu^2} (\mu e_x + e_y); \\ \tau &= G' \gamma. \end{aligned} \right\} \quad (28)$$

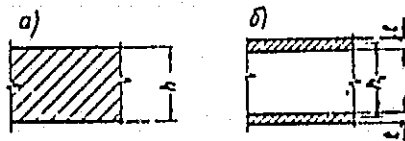


Fig. 7. Designed cross-sections of shells:  
a—single-layer; b—three-layer

By equating expression (27) and (28), we obtain

$$\mu = \frac{1}{3}; \quad E' = \frac{2EF}{\sqrt{3} h}; \quad G' = \frac{\sqrt{3} EF}{4h}. \quad (29)$$



$E'$  can be assumed to be equal to  $E$ ; then

$$I = \frac{2F}{\sqrt{3}l}; \quad G' = \frac{3}{8}E. \quad (30)$$

The three-layer spherical shells can easily be brought to a single-layer, if one disregards the deformations of shift of the filler—connective lattice.

The work of a connective lattice between two lattice surfaces of a spherical dome is evidently similar to the work of a lattice in flexible rods; based on known formulas of applied flexibility, one can draw the conclusion that the error introduced by such an assumption will be insignificant, if the ratio of the area of the working rod to the area of the rod of the lattice is small.

For a shell of solid cross-section (fig. 7, a), the bending and tensile rigidities are respectively equal to

$$D = \frac{Eh^3}{12(1-\mu^2)}; \quad B = \frac{Eh}{1-\mu^2}. \quad (31)$$

Similar expressions for a three-layer shell, with disregard for the inherent bending rigidity of the layers, have the form (fig. 7, b)

$$D_1 = \frac{E_1 h_1^3}{2(1-\mu_1^2)}; \quad B_1 = \frac{2E_1 h}{1-\mu_1^2}, \quad (32)$$

where  $h$ , is the distance between layers.

With the conditions of equality of the Poisson coefficients, equating expressions (31) and (32) and utilizing formula

(30), we obtain

ORIGINAL PAGE IS  
OF POOR QUALITY

$$h = \sqrt{3} h_1; \quad E = \frac{4E_1 F}{3h_1} \quad (33)$$

Thus, the formulas (33) make it possible to reduce the calculation of the rigidity of a three-layer lattice dome to calculation of the rigidity of some solid isotropic shell with a given thickness and modulus of elasticity.

/334

A feature of the problem of rigidity of thin-wall spherical shells consists of the fact that shape imperfections have a very great effect on the magnitude of the critical loads. The most unfavorable are local concavities on the surface of the shells, which corresponds in dimensions and profile to the bulging in the process of loss of rigidity. Numerous experimental investigations have established that the loss of rigidity of spherical shells takes place in a large range of specific loads  $\rho_0 = 0.6-0.2$  ( $\rho_0 = \rho_K \frac{R^2}{EK^2}$ ), with the relative magnitude of the maximum sag  $f_0/h$  being one of the basic parameters which determine the magnitude of the critical loads in this case; the critical pressures are lower the deeper the initial hollows on the shell.

The majority of theoretical investigations on rigidity of spherical shells has been devoted to the determination of that minimal load at which the shells do not lose rigidity with any deviations from the ideal shape. The problem was solved by the construction of a curve which determines the dependence of the magnitude of the maximum sag on the load on the shells. The minimum value of the load, the so-called lower critical pressure, was set equal to the desired magnitude of the load.

Such an approach to the solution of the problem was justified by the satisfactory coincidence of the results of the experimental and theoretical investigations, insofar as the least value of the lower critical pressure, obtained by Kh. M. Mushtari [1], was equal to  $p_0 = 0.22$ . However, in 1961, A. G. Gabril'yants and V. M. Fedos'ev published a numerical solution of nonlinear equations of a spherical shell, obtained on an electronic digital computer [2], where the lower critical load proved to be equal to 0.134, and corresponded to the sag, which exceeded the thickness of the shell by 22.5 times. With such large sags, it is impossible to consider the shape of the resilient hollow axisymmetric.

Numerous tests with spherical shells [3,4] show that, with sags  $f > 10h$ , a switch from a circular shape of bulging to a triangular shape is characteristic. The theoretical substantiation of the regularity of occurrence of a non-symmetric shape of the hollows in the supercritical stage is given in study [5].

Finally, the hypothesis of declivity of the area of bulging with large sags can also introduce substantial errors. Based on more general regularities, detached from this hypothesis, A. V. Pogorelov showed [6] that, for a resilient spherical shell, the lower critical load does not exist at all, since all of the resilient states are unstable with bulging. The experimentally determined lower critical load is a result of the occurrence of plastic deformations.

Thus, one can draw the conclusion that it is most correct to carry out engineering calculation of the rigidity of spherical shells according to the upper critical loads, obtained with regard for the initial sags. Such an approach, in addition to the apparent logic of posing of the problem,

more precisely corresponds to the initial hypotheses on the declivity and axisymmetry of the zone of bulging, as well as the assumption of the retention of the resilient properties of the material, insofar as the investigations are carried out in the range of small relative sags.

/335

However, such a method of solution, with respect to thin-walled sheet structures, can not yet be recommended, insofar as the designer does not have available sufficiently reliable data on the magnitude of the potential deviations from the correct shape. These deviations depend on many random factors, the differentiated calculation of which is presently impossible. For example, for a structure of a spherical gas tank, these factors may be: deviations in the thickness of the sheet during rolling and drop forging, inaccuracies of manufacture of the punches, errors during cutting, slight curvatures which form during transportation and assembly, welding deformations, and others. Even if one managed to determine the calculated magnitude of the initial cambers for each individual type of structure, on the basis of gathering of statistical data, one could hardly expect a substantial increase in the critical loads, as compared with the practical magnitudes obtained by experimental means.

Conversely, for large-span lattice shells and covers, the calculation of the rigidity, with regard for the initial deviations in shape, is uniquely correct, insofar as the relative magnitudes of these deviations, as compared with sheet structures which are small in size, should be considerably smaller. This assumption is based on one of the main corollaries of the theory of measurements, according to which the relative accuracy of measurement, and therefore also the accuracy of manufacture, increase in proportion to the increase in the dimensions. For example, with class 6 accuracy,

the allowance for the manufacture of the elements of metallic structures up to 1.5 m in length is 1.4 mm (relative accuracy of 1:1000), for those up to 33 m in length—8 mm (relative accuracy of 1:2400). In this case, it is necessary to take into account the fact that the relative thicknesses of two-layer lattice shells, calculated according to formula (33), may exceed by 10-20 times the relative thicknesses of thin-walled solid shells. Therefore, if the initial cambers in sheet structures at once reach on the order of one-two thicknesses of the shells, then, for large-span structures, the magnitude of the deviation should be considerably lesser.

On the other hand, for such relatively thin-walled shells, the concept of a lower critical pressure loses its practical sense, insofar as the area of plastic deformations corresponds unconditionally to cambers on the order of 20 thicknesses.

Utilizing statistical methods, we will evaluate the magnitude of the potential irregularities in the shape of three-layer lattice domes.

We will assume that the three-layer lattice dome is made up of one type of two-branch rods. The projected curvature of each product dome, consisting of individual rod branches of a single direction, is provided by the difference in the lengths of the upper and lower branches (fig. 8):

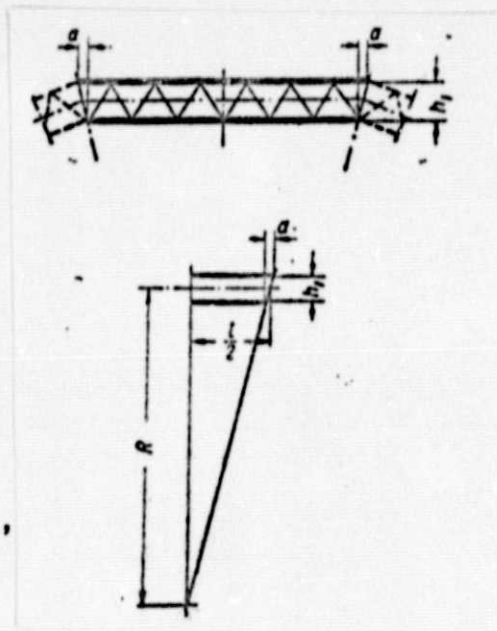


Fig. 8. Geometric diagram of two-branch rod of a dome framework

$$\frac{1}{R} = \frac{a}{lh_1},$$

where  $a = z_g - z_H$ .

As a result of errors in manufacture, the potential deviation in the magnitude of  $a$  is

$$\Delta a = \Delta l \sqrt{2}.$$

Here,  $\Delta l$  is the random error in the manufacture of a rod with a length  $l$ . As is common knowledge, the distribution of errors in the dimensions of linear elements corresponds quite accurately to Gauss' normal law of distribution.

We will assume that  $\Delta l$  corresponds to a certain number of

standards  $k = \frac{\Delta l}{\sigma}$ , with the proba-

bility of the occurrence of such an error being equal to  $\Phi$ . The additional difference in the lengths of the upper and lower branches in the section of the

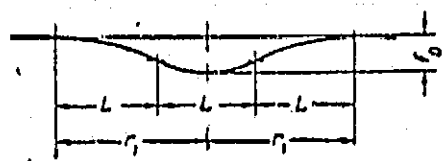


Fig. 9. Potential shape of initial curvature of product dome

generatrix  $L = m l$ , which is equal to

$$\Delta a = \frac{\Delta l \sqrt{2}}{\sqrt{m}} = k \sigma \sqrt{2 \frac{l}{L}}. \quad (34)$$

will correspond to this very same probability.

Consequently, as a result of the errors in manufacture of individual rods, the generatrix in section  $L$  may produce an additional curvature of the axis, with an average value of

curvature which is equal to

$$\kappa = \frac{\Delta a}{lh_1} = \frac{k\sigma}{lh_1} \sqrt{\frac{2l}{L}}. \quad (35)$$

We are interested in that curvature of the generatrix with which the surface of the dome takes on the shape of an axisymmetric hollow with a radius  $r_1$  (fig. 9).

The simplest shape of a curved line should have one section of positive curvature, and two sections of negative curvature. We will assume that all three sections have an equal length  $L=2/3 r_1$ , and an equal average curvature  $\kappa$ . By approximately assuming a uniform distribution of the curvature in the sections  $L$ , according to figure 9, we obtain

$$f_0 = \frac{5}{8} \kappa L^2 = \frac{5 \sqrt{2}}{8} \cdot \frac{k\sigma L \sqrt{L}}{h_1 \sqrt{L}} = \frac{5}{6 \sqrt{3}} k\sigma \frac{r_1 \sqrt{r_1}}{h_1 \sqrt{L}}. \quad (36)$$

We will also determine the probability  $\Phi$  of the occurrence of a given shape of the curvature of the generatrix.

Insofar as the probability of the occurrence on the generatrix of one section of curvature  $L$  equal to  $\Phi$ , then, according to the theory of multiplication of probabilities [7], the probability of the coincidence of three sections of the curvature, located next to one another, is

$$\Phi_1 = \Phi^3.$$

Errors in dimensions of  $\pm 3\sigma$  are considered maximum. The probability of the occurrence of errors of more than  $3\sigma$  is quite small—0.135%, and such errors are usually disregarded

/337

during the establishment of tolerances. By assuming, therefore, that  $\Phi_1 = 0.00136$ , we obtain  $\Phi = 0.111$ .  $k = 1.22$  corresponds to this probability. Consequently:

$$f_0 = 0.196 \frac{f_1 \sqrt{n}}{h_1 \sqrt{l}} \delta, \quad (37)$$

where  $\delta = 3\sigma$  is the permissible deviation in the rod length.

The curvature of one generatrix still does not mean the occurrence of a spatial hollow on the surface of the dome. A spatial hollow may occur only in that case when several adjacent generatrices, all in the same direction, have similar shapes of curvature. The probability of such an occurrence is on the order of

$$\Phi_2 = \Phi^n,$$

where  $n \approx \frac{2r_1}{0.872}$  is the number of generatrices in the section of the surface being examined.

However, such an approach may evidently lead to understated results.

We will think that the set of amplitudes of the deviations of all of the generatrices in an area of radius  $r_1$ , equal to  $f_0 \sqrt{n}$ , will be equivalent to the formation of a spatial concavity of the middle surface with a depth  $f_{0H}$ , equal to

$$f_{0H} = \frac{f_0 \sqrt{n}}{n} = \frac{f_0}{\sqrt{n}}. \quad (38)$$

By substituting formula (37) herein, we obtain



$$f_{0n} = 0,13 \frac{f_1}{h_1} \delta.$$

(39)

The initial sags of the shell have the greatest influence on the reduction of the upper critical load in that case when their dimensions coincide with the dimensions of the area of elastic bulging in the initial stage of the loss of rigidity. Therefore [8]:

$$r_1^2 \approx 9Rh \approx 9\sqrt{3}Rh_1.$$

Finally, we obtain

$$\xi_0 = \frac{f_{0n}}{h} = 0,3 \frac{\delta}{R} \left( \frac{R}{h_1} \right)^{\frac{3}{2}}. \quad (40)$$

Formula (40) shows that, with a constant ratio  $\frac{R}{h_1}$ , the relative initial sags decrease with an increase in the radius of curvature of the dome.

As is common knowledge, the upper critical load for a spherical shell, with the absence of initial deviations, is

$$p_k = \frac{2}{\sqrt{3(1-\mu^2)}} E \left( \frac{h}{R} \right)^3. \quad (41)$$

If the spherical shell has initial irregularities in shape, then the expression for the critical load has the form

/338

$$p_k = \frac{2}{\sqrt{3(1-\mu^2)}} \bar{p}_k E \left( \frac{h}{R} \right)^3. \quad (42)$$

Here,  $\bar{\rho}_k = \frac{\rho_k}{\rho_B}$  is the coefficient of reduction of the

upper critical load, as a function of the depth of the initial sags.

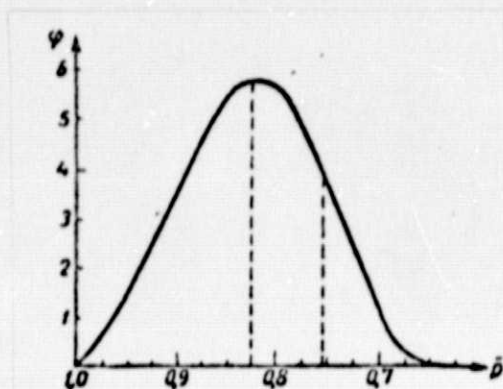


Fig. 10. Graph of the function of the distribution of the parameter of the critical load  $\bar{\rho}_k$  with  $3\sigma_{\xi_0} = 0.1$

By substituting the expressions for  $h$  and  $E$ , according to formula (33), into formula (42), we obtain

$$\rho_k = \frac{4\sqrt{3}}{\sqrt{2}} \bar{\rho}_k \frac{E_1 h_1 F}{IR^2}. \quad (43)$$

The effect of the initial sags on the magnitude of the upper critical load was investigated in study [8]. For small values of  $\xi_0 < 0.3$ , the function of the coefficient of reduction of the upper critical load

can be approximately written in the form

$$\rho_k = 1 - 0.925 \xi_0^{0.445}. \quad (44)$$

Utilizing expression (44), one can construct the function of the distribution of the critical load in a manner similar to that in study [7] for a cylindrical panel. Depicted in figure 10 is the function of distribution  $\varphi(\bar{\rho}_k)$  for  $3\sigma_{\xi_0} = 0.1$ . The mathematical expectancy proved to be equal to 0.825. As a result of conversion, the density increased considerably in the area of lesser magnitudes of  $\bar{\rho}_k$ , and the probability of a critical load  $\bar{\rho}_k > 0.668$ , which corresponds to  $\xi_0 = 0.1$ , proved to be considerably higher than the proba-

bility of initial sags  $\zeta = 0.1$ . It is evidently necessary to adopt  $\bar{\rho}_k = 0.658$ , corresponding to a probability of 0.0013, in the capacity of a calculation magnitude in the given case.

During the solution of concrete problems, knowing the conditions of manufacture of the structure being designed, one can obtain the magnitude of the initial sag from relationship (40), and then, utilizing the transformation of probabilities, determine the coefficient of reduction of the upper critical load and its probability characteristics. The critical load is determined according to formula (43).

For normal conditions of manufacture of metallic structures, adopting permissible deviation in rod length according to the Construction Norms and Specifications, it is not difficult to obtain that maximum ratio  $R/h$ , which guarantees total rigidity of three-layer lattice domes.

By setting formula (43) equal to the expression for the maximum load on a dome, from the condition of a supporting capability of the individual rods of

$$q = \frac{4 \sqrt{3} \sigma \varphi R}{Rl}, \quad (45)$$

we obtain

339

$$\frac{R}{h_1} = \frac{\bar{\rho}_k E_1}{\sqrt[3]{2 \sigma \varphi}}. \quad (46)$$

Here,  $\sigma$  is the calculated resistance of the material of the rods of the lattice dome;

$\varphi$  is the coefficient of longitudinal rigidity.

The calculations according to formulas (40) and (46) show that, for metallic two-lattice domes with  $R > 30$  m, the maximum ratio of  $R/h$ , can be assumed to be equal to

$$\frac{R}{h_1} = 300. \quad (47)$$

### Conclusions

1. Lattice domes with  $R > 30$  m should be designed as three-layer, in order to ensure their total rigidity.

2. Design of such domes can be carried out as single-layer solid shells, with given thicknesses and moduli of elasticity.

3. Insofar as the initial irregularities of shape of the lattice domes are small, calculation of the rigidity should be carried out according to the upper critical loads, with regard for accuracy of manufacture of individual rods of the elements.

4. For normal accuracy of manufacture, total rigidity is ensured with  $R/h_1 < 300$ .

REFERENCES

1. Mushtari, Kh. M., "K teorii ustoychivosti sfericheskoy obolochki pod deystviem vneshnego davleniya" [On the Theory of Rigidity of a Spherical Casing Under the Effect of External Pressure], in association with the articles of V. I. Fedos'ev, PMM, XIX, 2 (1955).
2. Gabril'yants, A. G., Fedos'ev, V. I., "Ob osesimmetrichnykh formakh ravnovesiya uprugoy sfericheskoy obolochki, nakhodyashchey pod deystviem ravnomerno raspredelennogo davleniya" [Axisymmetric Forms of Equilibrium of a Resilient Spherical Casings, Found Under the Effect of a Uniformly Distributed Pressure], PMM, XXV, 6 (1961).
3. Kloppel, K., Jungbluth, O., "Beitrag zum Durchschlagsproblem dünnwandiger Kugelschalen", Stahlbau, 22, 6 (1953).
4. Ashwell, D.G., "On the Large Deflection of a Spherical Shell with an Inward Point Load", Proceedings of IUTAM Symposium on the Theory of Thin Elastic Shells, Amsterdam, 1960.
5. Pogorelov, A. V., "Ob ustoychivosti osesimmetricheskikh deformatsiy sfericheskikh obolochek pri osesimmetricheskikh nagruzheniyakh" [The Rigidity of Axisymmetric Deformations of Spherical Casings with Axisymmetric Loadings], Doklady AN SSSR, 151, 5 (1963).
6. Pogorelov, A. V., K teorii vypuklykh-uprugikh obolochek v zakriticheskoy stadii [On the Theory of Convex Elastic Casings in the Supercritical Stage], Khar'kov University Publishing House, 1960.
7. Bolotin, V. V., Statisticheskie metody v stroitel'noi mekhanike [Statistical Methods in Construction Mechanics], Stroyizdat, Moscow, 1965.
8. Savel'ev, V. A., "Ob ustoychivosti sfericheskoy obolochki s nachal'nymi nepravil'nostyami formy sredinnoi poverkhnosti" [The Rigidity of a Spherical Casing with Initial Irregularities of the Shape of the Middle Surface], Inzhenernyy zhurnal, 5, 5 (1965).